European Journal of Chemistry

View Journal Online
View Article Online

Synthesis, antimicrobial, and antitubercular evaluation of new Schiff bases with *in silico* ADMET and molecular docking studies

Sakshith Raghavendra Prasad [1,2], Nayak Devappa Satyanarayan [2,*], Avarse Satish Kumar Shetty [1] and Basaiah Thippeswamy [3]

[1] *Department of Pharmaceutical Chemistry, National College of Pharmacy, Balaraj Urs Road, Shivamogga-577201, Karnataka, India*
[2] *Department of Pharmaceutical Chemistry, Kuvempu University, Post-Graduate Centre, Kadur-577548, Karnataka, India*
[3] *Department of Post-Graduation Studies and Research in Microbiology, Jnanasahyadri, Kuvempu University, Shankaraghatta-577451, India*

* *Corresponding author at: Department of Pharmaceutical Chemistry, Kuvempu University, Post-Graduate Centre, Kadur-577548, Karnataka, India.*
e-mail: satya1782005@gmail.com (N.D. Satyanarayan).

RESEARCH ARTICLE

10.5155/eurjchem.13.1.109-116.2216

Received: 18 November 2021
Received in revised form: 31 December 2021
Accepted: 03 January 2022
Published online: 31 March 2022
Printed: 31 March 2022

KEYWORDS

5V3Y
MABA
In silico
Antifungal activity
Multistep synthesis
Antibacterial activity

ABSTRACT

Schiff bases are a proven moiety in antitubercular drug discovery and the antitubercular drug development. Drug discovery is a never-ending process due to evolving drug resistance by the bacteria, as a result, there is a need of developing new antitubercular drugs. In this continuous process of antitubercular drug discovery, new series of Schiff bases are synthesized using quinoline carbohydrazide upon coupling with different aldehydes in ethanolic media through multistep synthesis. These synthesized compounds were purified and characterized by different spectroscopic techniques. The molecules were *in vitro* screened for antifungal and antibacterial potential by Agar well diffusion assay, antitubercular activity by using microplate Alamar blue assay, and an attempt has been made to study the *in-silico* relationship between new Schiff base derivatives 4a-f and the crystal structure of *M. tuberculosis* (5V3Y) protein by molecular docking studies. Synthesized compounds 4a-f show good interaction with the crystal structure of *M. tuberculosis* protein (5V3Y) and fulfill ADMET characteristics *in silico* experiments. Among the compounds tested, compound 4d was found to be active against bacteria and fungi. Compound 4b was found to be sensitive against *M. tuberculosis* at 50 µg/mL concentration.

Cite this: *Eur. J. Chem.* **2022**, *13(1)*, 109-116 **Journal website**: www.eurjchem.com

1. Introduction

Mycobacterium tuberculosis is a highly infectious airborne bacterium that causes tuberculosis (TB) disease and infects about 10 million people and kills over 1 million people each year [1]. Antitubercular drug design and development is one of the challenging research areas in the scientific forum, because of the limited efficacy and insufficiency of the drug options with their drawn-out duration of therapy, toxicity, high cost, and resistivity [2] in the current antitubercular treatment.

Schiff bases are molecules with a –C=N– group that are synthesized via the condensation of a primary amine and an aldehyde [3]. Schiff bases ligands are a type of molecule that have biological and pharmacological properties such as antibacterial, antifungal, and antitubercular properties [4,5]. Many studies on Schiff bases have been investigated as can be seen from the literature [6,7]. However, no work on this specific type of Schiff base has been envisaged. In search of bioactive structures, we investigated quinoline and its derivatives, which turned out as potent antimicrobial and, antitubercular moiety [8,9]. Quinoline derivatives containing Schiff bases have received attention due to their significant applications in medicine [10,11].

Considering the important features and facts of quinoline with Schiff base moiety, we welcomed and directed our research towards developing new compounds with similar structural features. In this work, the designed Schiff bases were synthesized from the condensation of quinoline carbohydrazide with different aldehydes and subsequently purified and characterized by different spectroscopic techniques. The molecules were *in vitro* screened for antifungal and antibacterial potential by Agar well diffusion assay, antitubercular activity by using microplate Alamar blue assay, and also an attempt has been made to study an *in-silico* relationship between new Schiff base derivatives **4a-f** and crystal structure of *M. tuberculosis* (5V3Y) protein by molecular docking studies.

2. Experimental

2.1. Material

2D structural models were drawn in ACD/ChemSketch software [12] and SMILES were generated for the molecules.

ISSN 2153-2249 (Print) / ISSN 2153-2257 (Online)
https://dx.doi.org/10.5155/eurjchem.13.1.109-116.2216

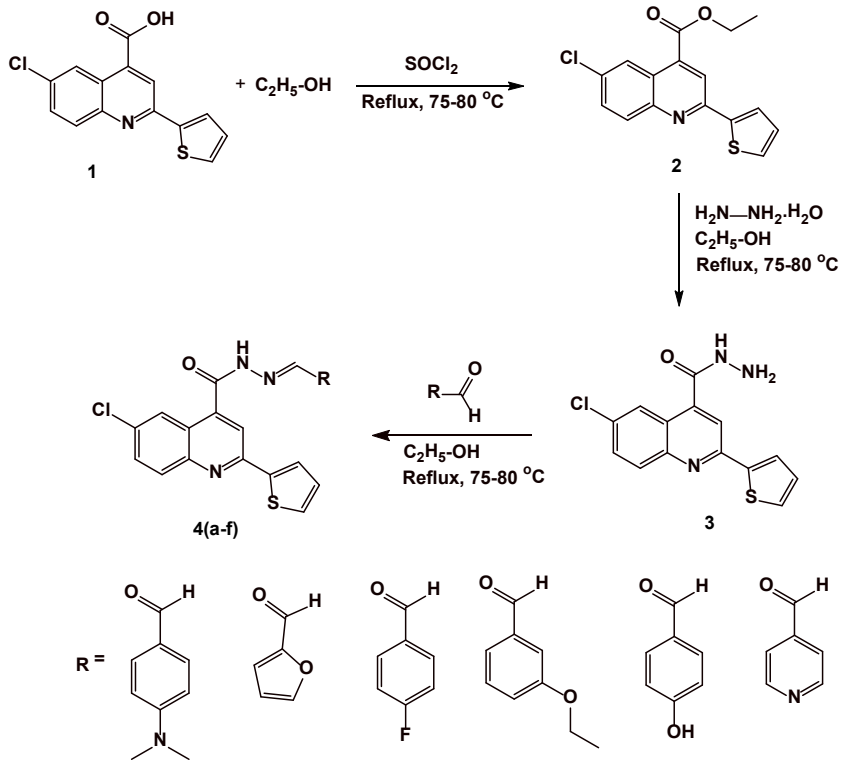

Scheme 1. Synthesis of 6-chloro-*N*'-methylidene-2-(thiophen-2-yl)quinoline-4-carbohydrazide derivatives (**4a-f**).

Individual ADME, bioactive, and drug-likeness scores were predicted for the designed molecules by online tools, admetSAR and molinspiration cheminformatics. Preparations of ligands were carried out by the Chimera docking tool [13]. The docking was done by the PyRx docking tool [14]. Visualization of the docked ligand and target protein interaction was carried out using Discovery studies 2020 [15]. Chemicals used for synthesis were from Sigma Aldrich, Spectrochem Pvt, Ltd. and Alfa Aesar. The solvents used for synthesis were distilled, and they were of reagent quality. Shimadzu LC-MS was used for mass spectroscopic analysis. TLC analysis was carried out on Merck 0.25 mm pre-coated silica gel $60F_{254}$ plates, and the spots were seen under UV light. The infrared data was obtained by Bruker spectrophotometer using the KBr pellet method. Bruker spectrometer were used with deuterated DMSO solvent and internal standard TMS to study ^{1}H and ^{13}C NMR spectra. For column chromatographic purification, Merck silica gel (100-200) mesh was utilised.

2.2. Synthesis

2.2.1. The starting material 2-thiophene quinoline-4-carboxylic acid (1)

To the mixture of 0.01 mol of 5-chloro isatin in 10 mL of ethanol and 10 mL of 33% KOH solution, 0.01 mol of 3-acetyl thiophene was added and kept for reflux for about 8 hours at 75-80 °C with a monitor of progress by TLC. After complete reflux, allowed to cool and pour onto the crushed ice slowly and neutralize by HCl solution. The separated solid was filtered, dried and recrystallized to yield compound **1** (Scheme 1) [16].

2.2.2. Synthesis of ethyl 6-chloro-2-(thiophen-2-yl) quinoline-4-carboxylate (2)

To the ethanol taken in a round bottom flask, thionyl chloride was added dropwise with constant stirring at 0 °C and followed by the addition of quinoline 4-carboxylic acid (**1**) and kept for reflux for about 8 hours at 75-80 °C with a monitor of progress by TLC. After complete reflux, allowed to cool and pour onto crushed ice slowly, neutralize by $NaHCO_3$ solution and the solid obtained was collected and purified by column chromatographic method to yield compound **2** (Scheme 1).

2.2.3. Synthesis of 6-chloro-2-(thiophen-2-yl)quinoline-4-carbohydrazide (3)

To the mixture of 0.01 mol of ethyl 6-chloro-2-(thiophen-2-yl)quinoline-4-carboxylate (**2**) in 10 mL of ethanol, 0.06 mol of hydrazine hydrate was added and kept for reflux for about 8 hours at 75-80 °C with a monitor of progress by TLC. After complete reflux, allow to cool and pour onto the crushed ice slowly and neutralize by HCl solution. The separated solid was filtered, dried and washed with diethyl ether to yield compound **3** (Scheme 1).

2.2.4. Synthesis of 6-chloro-N'-methylidene-2-(thiophen-2-yl)quinoline-4-carbohydrazides (4a-f)

6-Chloro-2-(thiophen-2-yl)quinoline-4-carbohydrazide (**3**) (0.02 mol) is dissolved in 10 mL of ethanol, to this 0.02 mol of different carboxylic aldehydes was added and followed by the addition of acetic acid in a catalytic amount, kept for reflux for 3 hours at 75-80 °C with a monitor of progress by TLC. After complete reflux, allowed to cool and pour onto crushed ice slowly and the solid obtained was collected and purified by column chromatographic method to yield compounds **4a-f** (Scheme 1).

6-Chloro-*N*'-{(*E*)-[4-(dimethylamino)phenyl]methylidene} -2-(thiophen-2-yl)quinoline-4-carbohydrazide (**4a**): Color: Yellow amorphous. Yield: 82%. M.p.: 164-166 °C. FT-IR (KBr, ν, cm^{-1}): 3450 (N-H), 1650 (C=N), 1600 (C=C), 1550 (C=O), 1370 (CH_3), 750 (C-S), 600 (C-Cl). ^{1}H NMR (500 MHz, DMSO-d_6, δ, ppm): 3.150 (s, 6H, N-$(CH_3)_2$), 6.316 (m, 2H, J = 7 Hz, Ar-H),

6.632 (d, 1H, *J* = 9.2 Hz, Ar-H), 6.817 (t, 1H, *J* = 8 Hz, Ar-H), 7.042 (m, 2H, *J* = 8.5 Hz, Ar-H), 7.204 (d, 1H, *J* = 8.2 Hz, Ar-H), 7.577 (t, 1H, *J* = 10 Hz, Ar-H), 7.813 (d, 1H, *J* = 9.5 Hz, Ar-H), 8.212 (s, 1H, N=CH), 8.525 (s, 1H, Ar-H), 11.225 (s, 1H, NH). ^{13}C NMR (100 MHz, DMSO-d_6, δ, ppm): 37.66 ((-CH_3)$_2$), 111.50, 119.20, 126.08, 126.57, 127.24, 128.04, 128.59, 128.74, 129.21, 129.40, 130.79, 132.02, 134.24, 142.50, 144.82, 145.65, 151.45, 152.90 (Ar-C), 162.50 (C=O). MS (EI, *m/z* (%)): 435.09 (M+1).

6-Chloro-*N*'-[(*E*)-(furan-2-yl) methylidene]-2-(thiophen-2-yl)quinoline-4-carbohydrazide (**4b**): Color: Pale green amorphous. Yield: 83%. M.p.: 180-182 °C. FT-IR (KBr, ν, cm^{-1}): 3460 (N-H), 1710 (C=N), 1620 (C=C), 1520 (C=O), 1100 (C-O-C), 745 (C-S), 600 (C-Cl). ^{1}H NMR (500 MHz, DMSO-d_6, δ, ppm): 6.324 (t, 1H, *J* = 3.4 Hz, Ar-H), 6.632(d, 1H, *J* = 4 Hz, Ar-H), 6.817 (t, 1H, *J* = 7.5 Hz, Ar-H), 7.034 (d, 1H, *J* = 4 Hz, Ar-H), 7.068 (d, 1H, *J* = 8 Hz, Ar-H), 7.204 (d, 1H, *J* = 8 Hz, Ar-H), 7.572 (t, 1H, *J* = 7 Hz, Ar-H), 7.601 (s, 1H, Ar-H), 7.813 (d, 1H, *J* = 9.5 Hz, Ar-H), 8.212 (s, 1H, N=CH), 8.525 (s, 1H, Ar-H), 11.225 (s, 1H, NH). ^{13}C NMR (100 MHz, DMSO-d_6, δ, ppm): 109.50, 112.48, 119.22, 126.02, 126.54, 127.26, 128.02, 128.51, 128.72, 129.25, 130.77, 132.03, 134.87, 139.33, 143.24, 145.56, 147.82, 152.94 (Ar-C), 161.10 (C=O). MS (EI, *m/z* (%)): 382.03 (M+1).

6-Chloro-*N*'-[(*E*)-(4-fluorophenyl) methylidene]-2-(thiophen-2-yl)quinoline-4-carbohydrazide (**4c**): Color: Pale yellow amorphous. Yield: 78%. M.p.: 150-152 °C. FT-IR (KBr, ν, cm^{-1}): 3480 (N-H), 1690 (C=C), 1600 (C=N), 1500 (C=O), 1490 (C-F), 749 (C-S), 600 (C-Cl). ^{1}H NMR (500 MHz, DMSO-d_6, δ, ppm): 6.328 (m, 2H, *J* = 8 Hz, Ar-H), 6.751 (d, 1H, *J* = 9 Hz, Ar-H), 6.817 (t, 1H, *J* = 7.4 Hz, Ar-H), 7.061 (m, 2H, *J* = 8 Hz, Ar-H) 7.207 (d, 1H, *J* = 4 Hz, Ar-H) 7.565 (d, 1H, *J* = 7.5 Hz, Ar-H), 7.601 (s, 1H, Ar-H), 7.816 (d, 1H, *J* = 4 Hz, Ar-H), 8.252 (s, 1H, N=CH), 8.555 (s, 1H, Ar-H), 11.204 (s, 1H, NH). ^{13}C NMR (100 MHz, DMSO-d_6, δ, ppm): 116.70, 120.38, 127.28, 128.34, 128.91, 129.43, 129.89, 130.40, 131.48, 131.80, 133.10, 135.95, 140.63, 145.47, 147.10, 146.83, 152.77, 155.80, 156.03, 156.10 (Ar-C), 166.24 (C=O). MS (EI, *m/z* (%)): 410.04 (M+1).

6-Chloro-*N*'-[(*E*)-(3-ethoxyphenyl) methylidene]-2-(thiophen-2-yl)quinoline-4-carbohydrazide (**4d**): Color: Off white amorphous. Yield: 77%. M.p.: 168-170 °C. FT-IR (KBr, ν, cm^{-1}): 3400 (N-H), 1680 (C=C), 1640 (C=N), 1550 (C=O), 1200 (C-O-C), 720 (C-S), 610 (C-Cl). ^{1}H NMR (500 MHz, DMSO-d_6, δ, ppm): 2.478 (s, 3H, -CH_3), 4.449 (m, 2H, *J* = 6.5 Hz, O-CH_2-), 7.107 (t, 2H, *J* = 6 Hz, Ar-H), 7.8188 (d, 1H, *J* = 6.5 Hz, Ar-H), 7.899 (d, 2H, *J* = 6.5 Hz, Ar-H), 8.000 (d, 2H, *J* = 12.5 Hz, Ar-H), 8.130 (d, 1H, *J* = 5 Hz, Ar-H), 8.216 (s, 1H, N=CH), 8.322 (s, 1H, Ar-H), 8.394 (s, 1H, Ar-H), 8.688 (s, 1H, Ar-H), 11.401 (s, 1H, NH). ^{13}C NMR (100 MHz, DMSO-d_6, δ, ppm): 14.89 (-CH_3), 65.12 (O-CH_2-), 115.18, 116.94, 122.56, 124.93, 125.67, 127.28, 127.54, 127.86, 129.72, 130.22, 131.87, 133.45, 139.56, 141.56, 144.83, 152.94, 158.51 (Ar-C), 161.93 (C=O). MS (EI, *m/z* (%)): 436.07 (M+1).

6-Chloro-*N*'-[(*E*)-(4-hydroxyphenyl) methylidene]-2-(thiophen-2-yl)quinoline-4-carbohydrazide (**4e**): Color: Pale yellow amorphous. Yield: 68%. M.p.: 160-162 °C. FT-IR (KBr, ν, cm^{-1}): 3600 (-OH), 3400 (N-H), 1660 (C=C), 1622 (C=N), 1510 (C=O), 730 (C-S), 670 (C-Cl). ^{1}H NMR (500 MHz, DMSO-d_6, δ, ppm): 5.019 (s, 1H, -OH), 6.329 (t, 2H, *J* = 8 Hz, Ar-H), 6.636 (d, 1H, *J* = 7.5 Hz, Ar-H), 6.817 (t, 1H, *J* = 8.3 Hz, Ar-H), 7.034 (m, 2H, *J* = 7.5 Hz, Ar-H), 7.566 (d, 1H, *J* = 4Hz, Ar-H), 7.601 (s, 1H, Ar-H), 7.814 (d, 1H, *J* = 8.4 Hz, Ar-H), 8.252 (s, 1H, N=CH), 8.523 (s, 1H, Ar-H), 11.274 (s, 1H, NH). ^{13}C NMR (100 MHz, DMSO-d_6, δ, ppm): 115.68, 117.63, 118.06, 121.94, 125.81, 126.58, 127.45, 127.66, 127.82, 129.06, 129.84, 131.12, 131.64, 134.91, 138.83, 141.75, 144.86, 152.67, 154.21 (Ar-C), 164.25 (C=O). MS (EI, *m/z* (%)): 408.05 (M+1).

6-Chloro-*N*'-[(*E*)-(pyridin-4-yl) methylidene]-2-(thiophen-2-yl)quinoline-4-carbohydrazide (**4f**): Color: Pale yellow amorphous. Yield: 71%. M.p.: 176-178 °C. FT-IR (KBr, ν, cm^{-1}): 3490 (N-H), 1690 (C=N), 1600 (C=C), 1520 (C=O), 730 (C-S), 690 (C-Cl). ^{1}H NMR (500 MHz, DMSO-d_6, δ, ppm): 7.001 (d, 2H, *J* = 9.5 Hz, Ar-H), 7.120 (t, 1H, *J* = 8 Hz, Ar-H), 7.301 (d, 2H, *J* = 8 Hz, Ar-H), 7.600 (d, 1H, *J* = 9 Hz, Ar-H), 7.775 (d, 1H, *J* = 6 Hz, Ar-H), 7.947 (d, 1H, *J* = 6.6 Hz, Ar-H), 8.206 (d, 1H, *J* = 8.5 Hz, Ar-H), 8.266 (s, 1H, N=CH), 8.378 (s, 1H, Ar-H), 8.412 (s, 1H, Ar-H), 8.868 (s, 1H, Ar-H), 11.351 (s, 1H, NH). ^{13}C NMR (100 MHz, DMSO-d_6, δ, ppm): 116.54, 121.78, 121.21, 125.37, 126.53, 127.27, 127.88, 128.18, 129.06, 130.24, 131.89, 134.15, 139.87, 141.53, 144.81, 149.62, 152.49 (Ar-C), 162.85 (C=O). MS (EI, *m/z* (%)): 393.05 (M+1).

2.3. Biological activity

2.3.1. Molecular docking

The molecules were drawn and the corresponding smile notations were generated using ACD-ChemSketch freeware software [12], and these smile notations were used to prepare the ligands for docking studies by USCF chimera tool [13]. The crystal structure of *M. tuberculosis* (PDB ID:5V3Y) was taken as macromolecule/protein for docking was obtained from online data server Protein Data Bank [17], prepared and converted to PDB format using USCF chimera tool. These prepared ligands were docked against protein using PyRX workstation's Autodock Vina [14] where the grid box is placed around the active site of the macromolecule and this active site was identified by the Uniport chimera tool. Using Schrödinger PyMol [18], the docked protein and ligands were saved in PDB format, and interactions were visualized using Biovia Discovery studios [19].

2.3.2. ADMET studies

The *in silico pharmacokinetic* parameters of the compounds were predicted by the online tool, admetSAR [20] and the drug likeness and bioactive scores were predicted by the online tool, Molinspiration cheminformatics [21]. The 2D structural models of the designed molecules were drawn on ACD/ChemSketch software and SMILES were generated for the molecules along with standard drugs, these smiles notations were used for predicting the individual ADMET, bioactive and drug likeness scores. AdmetSAR gives data for the evaluation of active molecules and also for the removal of biologically defective major molecules with unwanted functional groups. The overall analysis of the significant molecules involves geometry, surface area, and fingerprint properties, which determine the biological significance of the region in a molecule. CACO-2 cell permeability, intestinal absorption, water solubility, hepatotoxicity, and blood-brain barrier penetration were the other parameters that helps to understand the metabolic drug mechanism of the designed molecules.

2.3.3. Antibacterial activity

The potential of the synthesized compounds **4a**-**f** to inhibit the pathogenic bacteria *Escherichia coli, Klebsiella pneumonia* and *Staphylococcus aureus*, *Salmonella typhimurium* were determined by Agar well diffusion assay [22,23]. The test bacteria were aseptically injected into sterile nutrient broth tubes and cultured at 38 °C for 24 hours in this technique. The 24 hours old liquid bacterial cultures were swab inoculated on sterile nutrient agar plates. In the inoculated plates, 6mm diameter wells were punched using sterile gel borer. Standard antibiotic (Chloramphenicol, 5 mg/mL of sterile distilled water (positive control)) prepared. A 100 µL of compound solutions and standard antibiotic solution were transferred aseptically into labelled wells. Sample loaded plates were not disturbed for 30 min and then incubated in the upright position for 24 hours at 38 °C. The inhibited zones developed around the wells were measured using a zone scale or ruler.

Table 1. Docking results of synthesized compounds **4a-f** Schiff bases with 5V3Y.

Compound	Hydrogen bond interactions	Hydrogen Bond's length in Å	Binding affinity in kcal/mol	Electrostatic interactions	Other interactions
4a	PRO1595 ALA1596	3.96 5.21	-9.1	PRO1598, ILE1594, VAL1614, TRF1579, VAL1611, TYR1582, PHE1585, PHE1670	PHE1613, LEU1602, ALA1583, ILE1597, ALA1586, TYR1637
4b	-	-	-8.6	PHE1585, MET1669, TYR1637, TRP1579, ALA1583, ILE1594, ALA1586	PHE1670, VAL1611, VAL1614, ILE1597, TYR1582
4c	PRO1598	4.70	-9.2	PHE1585, PHE1670, TYR1582, VAL1611, TRP1579, VAL1614	PRO1595, LEU1602, ALA1583, ILE1594, ALA1586, TYR1637
4d	-	-	-9.0	PHE1585, PHE1670, TYR1637, VAL1614, ILE1594, ALA1583	THR1589, LYS1588, PHE1590, VAL1611, TRP1579, ILE1597
4e	TYR1582	5.01	-9.5	PHE1585, MET1669, PHE1670, TRP1579, ILE1597, ALA1583, VAL1614	VAL1618, ALA1586, LEU1615, ILE1625
4f	-	-	-8.7	VAL1614, TRP1579, VAL1611, TYR1637, PHE1585, PHE1670	ILE1597, ALA1583, ILE1594, ALA1586, TYR1637, PRO1598, LEU1602

The size of the zone indicates the effectiveness of the compound towards pathogenic bacteria.

2.3.4. Anti-fungal activity

The potential of the synthesized compounds **4a-f** to inhibit the pathogenic fungi *Aspergillus niger* and *Aspergillus flavus* were determined by Agar well diffusion assay [24,25]. In this assay, the fungal spore suspension was prepared by inoculating loop full of fungal culture was inoculated into the 5 mL sterile water taken in test tube amended with 2 drops of an emulsifying agent; between 80. Test fungal spore suspensions were swabs inoculated on sterile Rose Bengal agar plates, and 6mm wells were punched in the inoculation plates with a sterile gel borer. Standard antifungal (Fluconazole, 10 mg/mL in sterile distilled water (positive control)) prepared. A 100 µL of 10 mg/mL concentration compound solution and standard antifungal solution were transferred aseptically into labeled wells. Sample loaded plates were not disturbed for 30 min and then incubated in the upright position for 72 hours at 28 °C. The inhibited zones developed around the wells were measured using a zone scale or ruler. The size of the zone indicates the effectiveness of the compound towards pathogenic fungi.

2.3.5. Anti-tubercular activity

The thermally stable and nontoxic microplate Alamar blue assay (MABA) method [26] was adopted to screen the title compounds **4a-f** against *M. tuberculosis* H37RV strain at a concentration from 0.8 to 100 µg/mL in a sterile 96 well plate. Deionized sterile water (200 µL) was added to the outer perimeter well to avoid evaporation. 100 µL of Middle brook 7H9 broth and serial dilutions of the compounds were introduced to the 96 wells plate and incubated at 36 °C for 120 hours. The sensitive compounds exhibited blue colour after 24 hours incubation against *M. tuberculosis* H37RV strain and the concentrations were recorded.

3. Results and discussion

3.1. Chemistry

The most efficient method for the synthesis of compounds **4a-f** was performed, 2-thiophen quinoline 4-carbohydrazide reacted with different aldehydes (4-dimetyl amine benzaldehyde, furfuran, 4-fluro benzaldehyde, 4-ethoxy benzadehyde, 4-hydroxy benzaldehyde and 4-carboxyldehyde pyridine) in ethanol as solvent and catalytic amount of acetic acid. The results are summarized in Scheme 1. The synthesized molecules were purified by column chrmotagraphy using twenty percent of ethyl acetate in *n*-hexane as eluent. Analytical TLCs were performed using twenty percent ethyl acetate in n-hexane as the eluent on precoated Merck 0.25 mm silica gel $60F_{254}$ plates, and the spots on developed TLC plates were identified under UV light. The structure of the molecules was characterized by IR, ^{1}H NMR, ^{13}C NMR, and mass spectroscopic techniques. The synthesized compounds **4a-f** were showed absorption bands ranging from 600-690 cm^{-1} for C-Cl stretching, 720-750 cm^{-1}for C-S stretching, 1500-1550 cm^{-1} for C=O stretching, 1600-1700 cm^{-1} for C=N stretching, and C=C aromatic stretching, 3400-3500 cm^{-1} for N-H stretching. In ^{1}H NMR spectra, the aliphatic protons appeared in the range between δ 2.1 and 5.5 ppm, aromatic protons appeared in the range of δ 6.5-8.8 ppm and NH protons appeared in the range of δ 11.2-11.4 ppm, in ^{13}C NMR all the aromatic carbon appeared in a range of δ 100-170 ppm.

3.2. Molecular docking

In silico molecular docking studies of the synthesized compounds against the crystal structure of *M. tuberculosis* (5V3Y) protein. The binding affinity of ligands and protein varies from -8.6 to -9.5 Kcal/mol, compound **4e** shows a greater binding affinity of -9.5 Kcal/mol and others also with good binding affinity varies from -8.6 to -9.2 Kcal/mol, compounds **4a**, **4c**, and **4e** show H-bond interaction with PRO1595, ALA1596, PRO1598, and TYR1582. The synthesized compounds show electrostatic interactions with PHE1585, PHE1670, TYR1582, VAL1611, TRP1579, and VAL1614. Binding modes and visual interaction are shown in Figure 1 and docking results are discussed in Table 1.

3.3. In-silico pharmacokinetic properties

3.3.1. ADMET studies

Pharmacokinetic ADME properties are one of the main descriptors in drug discovery for human therapeutic use. These ADME descriptor properties were calculated for the molecules with biological importance and are compared with the ranges acquired for standard drugs. The synthesized compounds **4a-f** do possess a considerable degree of hydrogen bond donors and acceptors as recorded through *in silico* data [27]. The derivatives were designed in such a way to acquire an increase in the binding capacity with that of the receptors through hydrogen bonding. The molecules synthesized accept Lipinski's rule 5 for oral bioavailability and character which enhances their chance to be considered as future drug candidates. The estimated Caco-2 permeability and BBB coefficient (log BB) were used to determine the total distribution of compounds in the human body, and the calculated BBB values were found to be within acceptable limits. The ADMET parameters of the synthesized compounds are shown in Table 2.

The toxicity of compounds **4a-f** is estimated based on lethal doses and their functioning ranges on various organs/tissues. Table 3 shows the probability of health consequences and the LD_{50} values that were predicted.

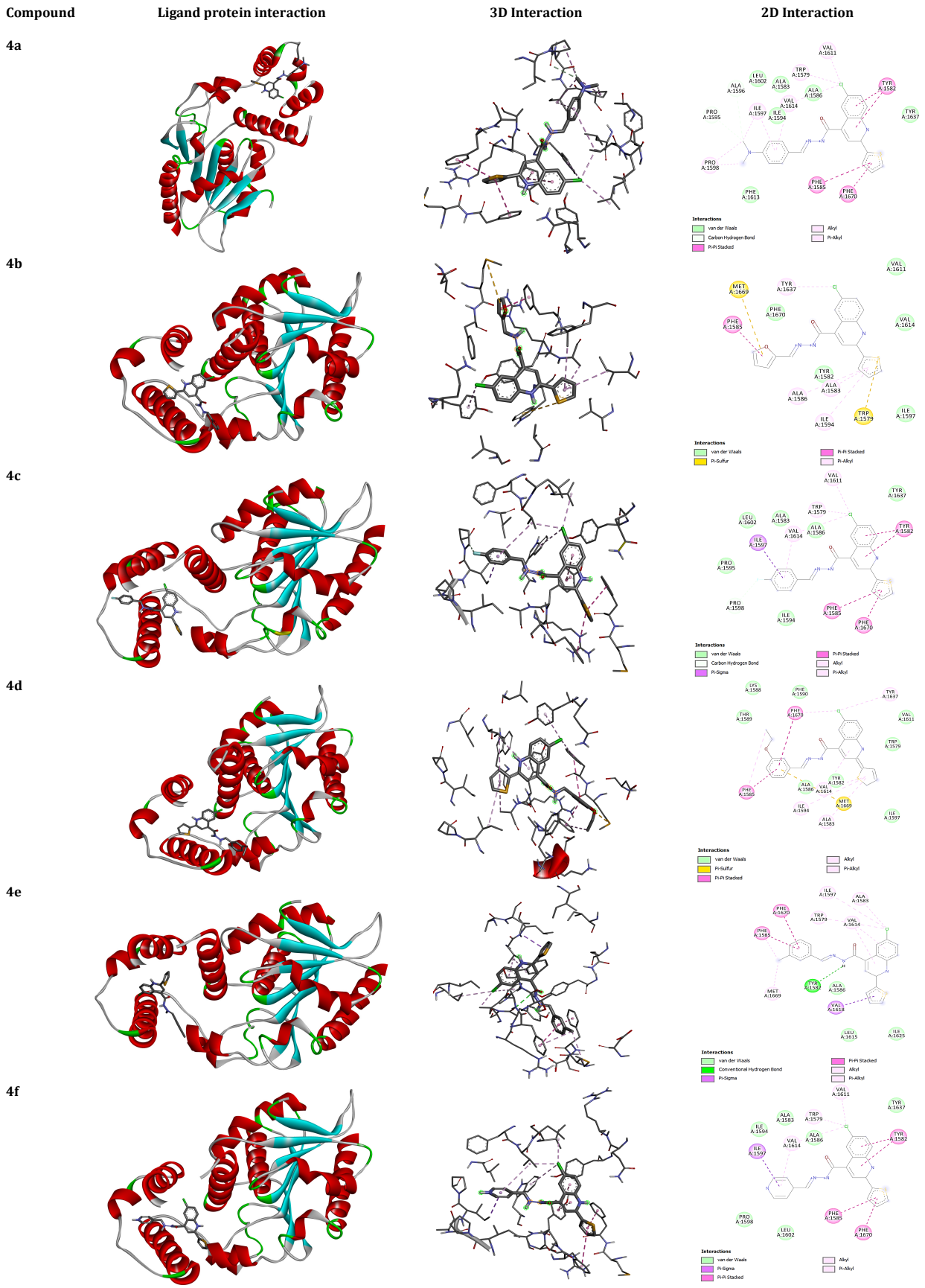

Figure 1. Interaction of synthesized compounds **4a**-**f** Schiff bases with 5V3Y.

Table 2. Predicted ADME and pharmacological characteristics of the synthesized compounds **4a**-**f**.

Compounds	Log BB	Log $_{HIA}$	Caco-2	Substrate log pGI	Non-inhibitor log PGI	Log S	Log papp
4a	0.8974	0.9912	0.5439	0.8215	0.8492	-3.6424	1.1402
4b	0.9524	1.0000	0.5783	0.7306	0.9343	-3.8535	0.8974
4c	0.9806	1.0000	0.5307	0.7924	0.8376	-3.7333	1.0494
4d	0.9848	1.0000	0.5407	0.7916	0.7742	-3.6350	0.9936
4e	0.8940	1.0000	0.5571	0.7572	0.9149	-4.1081	1.1227
4f	0.9114	1.0000	0.5000	0.6685	0.6090	-3.4684	1.0327
Chloramphenicol	0.9382	0.9871	0.7250	0.7313	0.9019	-2.1694	0.9184
Fluconazole	0.9382	0.9894	0.8867	0.6008	0.8782	-1.8626	1.3598
Isoniazid	0.9895	0.9892	0.6959	0.8315	0.9778	-0.0521	1.2413

Table 3. TOX parameters for the synthesized ligands.

TOX parameters	LD_{50}	Human hepatotoxicity	Mutagenicity	Skin sensitization
4a	1353.201	Yes	Yes	Yes
4b	1424.081	Yes	No	No
4c	1258.183	Yes	No	No
4d	1269.549	Yes	No	No
4e	1481.643	Yes	No	No
4f	1237.204	Yes	No	No

Table 4. Drug likeness score for the synthesized ligands.

Compounds	MW	mi LogP	TPSA	Number of atoms	Number of ON	Number of OHNH	Violations	Rotatable bonds
4a	434.95	5.76	57.59	30	5	1	1	5
4b	381.84	4.92	67.49	26	5	1	0	4
4c	409.87	5.83	54.35	28	4	1	1	4
4d	435.94	6.10	63.59	30	5	1	1	6
4e	405.91	6.09	54.35	28	4	1	1	4
4f	392.87	4.37	67.25	27	5	1	0	4
Chloramphenicol	323.13	0.73	115.38	20	7	3	0	6
Fluconazole	306.28	-0.12	81.66	22	7	1	0	5
Isoniazid	137.14	-0.97	68.01	10	4	3	0	1

Table 5. Bioactive score for the synthesized ligands.

Compounds	GPCR	Ion channel modulators	Kinase inhibitors	Nuclear receptors	Protease inhibitors	Enzyme inhibitor
4a	-0.51	-0.71	-0.37	-0.56	-0.63	-0.47
4b	-0.32	-0.66	-0.17	-0.43	-0.52	-0.28
4c	-0.36	-0.69	-0.20	-0.55	-0.53	-0.33
4d	-0.35	-0.70	-0.18	-0.53	-0.55	-0.34
4e	-0.33	-0.71	-0.19	-0.46	-0.47	-0.29
4f	-0.34	-0.67	-0.16	-0.51	-0.53	-0.33
Chloramphenicol	-0.22	-0.28	-0.38	-0.41	-0.21	-0.00
Fluconazole	0.04	0.01	-0.09	-0.23	-0.09	0.03
Isoniazid	-1.39	-1.45	-1.05	-2.33	-1.23	-0.66

Table 6. Inhibited zone's diameter in mm against bacteria.

Compounds	*Escherichia coli*	*Klebsiella pneumoniae*	*Staphylococcus aureus*	*Salmonella typhimurium*
4a	3	5	2	3
4b	4	4	4	4
4c	5	3	4	4
4d	6	7	5	4
4e	2	3	1	2.5
4f	3	5	2	3
Chloramphenicol	14	17	18	15
DMSO	0	0	0	0

3.3.2. Bioactivity and drug-likeness scores of synthesized compounds 4a-f

The five rules of Lipinski's are used predominantly by drug discovery teams in designing a drug and their development for their oral bioavailability. The rule insists that a drug candidate is to be orally active: i) Molecular weight should be less than 500 g/mol, ii) Hydrogen bond acceptors should be less than ten, iii) The partition coefficient should be less than five, iv) TPSA should be less than 160 Å and, v) Hydrogen bond donors should be less than five. None of the analogs have violated any rules of Lipinski and can be expected to be active orally. The molecular weights of **4a**-**f** are below 500 and are expected to be transported, diffused and absorbed across the membranes pretty easily than the macromolecules. The synthesized compounds **4a**-**f** correspond to the Lipinski rule. TPSA data of the molecules which are correlated with hydrogen bonding and are an indicator for bioavailability orally as the data is in the range of 64.70 to 110.52 Å well below 160 Å the limit (Table 4).

Molinspiration cheminformatics is the software approach to predict the bioactivity score of the synthesized compounds **4a**-**f** for drug targets and is represented in Table 5. Different pathways, such as interactions with inhibiting protease, nuclear receptor ligands, GPCR ligands, and other enzymes, are involved in the physiological functions obtained from synthesized molecules. The data also show that there is substantial interaction between the molecules and the drug targets. Molecules have shown a strong bioactivity score.

3.4. Antibacterial activity

The potential of synthesized compounds **4a**-**f** to inhibit the pathogenic bacteria was determined by Agar well diffusion assay (Table 6). In this study, *Escherichia coli, Klebsiella pneumonia* and *Staphylococcus aureus, Salmonella typhimurium* were selected because of their infectious nature. The study found that among the compounds tested, all the synthesized compounds **4a**-**f**, concerning antibacterial activities, compound **4d** shows potency against *E. coli* and *K. pneumonia.*

Table 7. Inhibited zone's diameter in mm against fungi.

Compounds	*Aspergillus niger*	*Aspergillus flavus*
4a	8	8.5
4b	8	10.5
4c	9	9
4d	10	10
4e	9.5	9.5
4f	10	10
Fluconazole	19.5	25
DMSO	0	0

Table 8. The antitubercular MIC values are expressed in µg/mL.

Samples	MIC (µg/mL)
4a	100±0.5
4b	50±0.5
4c	100±0.5
4d	100±0.5
4e	100±0.5
Pyrazinamide	3.125±0.20
Ciprofloxacin	3.125±0.20
Streptomycin	6.250±0.12

3.5. Antifungal activity

The potential of synthesized compounds **4a-f** to inhibit the pathogenic fungi *Aspergillus niger* and *Aspergillus flavus* were determined by Agar well diffusion assay. The study found that among the compounds tested, compound 4d shows good activity against the fungi *Aspergillus niger* and all other compounds show considering activity against *Aspergillus niger* and *Aspergillus flavus.* The *antifungal* activity of compounds **4a-f** is shown in Table 7.

3.6. Antitubercular activity

The synthesized compounds **4a-f** were screened against *M. tuberculosis* using microplate Alamar Blue assay (MABA). The study found that among the compounds tested, concerning antitubercular activities, the synthesized compounds **4a-f** were found to be sensitive against *M. tuberculosis* at a concentration of 100 µg/mL concentration, and compound 4b shows sensitivity at 50 µg/mL concentration. The antitubercular activity of the compounds is shown in Table 8.

4. Conclusion

A new series of Schiff bases were synthesized in the most efficient multistep route with good yield and screened for *in vitro* antimicrobial activity along with the antitubercular activity**.** The title compounds *in silico* studies have been determined to comply with ADME studies and Lipinski's five requirements. The docked ligands against the protein 5V3Y vary a binding affinity from -8.6 to -9.5 Kcal/mol, compound 4e shows a greater binding affinity of -9.5 Kcal/mol among all other also compounds. The antimicrobial study reveals that among the compounds **4a-f** tested, compound **4d** was found to be active against test bacteria and fungi with a greater zone of inhibition but comparatively lower to standard drug. The antitubercular activity reveals that among the tested compounds **4a-f**, compound **4b** shows sensitivity at 50 µg/mL concentration but not as good as standard. The compounds **4b** and **4d** can be taken as lead molecules where they can be further modified and developed to achieve the good activity.

Acknowledgements

The authors are grateful to the officials of Kuvempu University that they have provided the necessary facilities to carry out the present work.

Disclosure statement

Conflict of interests: The authors declare that they have no conflict of interest.

Ethical approval: All ethical guidelines have been adhered.
Sample availability: Samples of the compounds are available from the author.

CRediT authorship contribution statement

Conceptualization: Nayak Devappa Satyanarayan; Methodology: Sakshith Raghavendra Prasad; Validation: Avarse Satish Kumar Shetty; Data Curation: Basaiah Thippeswamy; Writing - Original Draft: Sakshith Raghavendra Prasad; Writing - Review and Editing: Nayak Devappa Satyanarayan; Supervision: Nayak Devappa Satyanarayan, Avarse Satish Kumar Shetty.

ORCID and Email

Sakshith Raghavendra Prasad
prasadsakshith@gmail.com
https://orcid.org/0000-0003-4700-1679
Nayak Devappa Satyanarayan
satya1782005@gmail.com
https://orcid.org/0000-0003-4511-3749
Avarse Satish Kumar Shetty
skshettyncp@gmail.com
https://orcid.org/0000-0003-2903-7678
Basaiah Thippeswamy
thippeswamyb205@gmail.com
https://orcid.org/0000-0002-6436-0289

References

[1]. Alsayed, S. S. R.; Lun, S.; Bailey, A. W.; Suri, A.; Huang, C.-C.; Mocerino, M.; Payne, A.; Sredni, S. T.; Bishai, W. R.; Gunosewoyo, H. Design, synthesis and evaluation of novel indole-2-carboxamides for growth inhibition of Mycobacterium tuberculosis and paediatric brain tumour cells. *RSC Adv.* **2021**, *11*, 15497–15511.
[2]. Dheda, K.; Gumbo, T.; Maartens, G.; Dooley, K. E.; McNerney, R.; Murray, M.; Furin, J.; Nardell, E. A.; London, L.; Lessem, E.; Theron, G.; van Helden, P.; Niemann, S.; Merker, M.; Dowdy, D.; Van Rie, A.; Siu, G. K. H.; Pasipanodya, J. G.; Rodrigues, C.; Clark, T. G.; Sirgel, F. A.; Esmail, A.; Lin, H.-H.; Atre, S. R.; Schaaf, H. S.; Chang, K. C.; Lange, C.; Nahid, P.; Udwadia, Z. F.; Horsburgh, C. R., Jr; Churchyard, G. J.; Menzies, D.; Hesseling, A. C.; Nuermberger, E.; Mcllleron, H.; Fennelly, K. P.; Goemaere, E.; Jaramillo, E.; Low, M.; Jara, C. M.; Padayatchi, N.; Warren, R. M. The epidemiology, pathogenesis, transmission, diagnosis, and management of multidrug-resistant, extensively drug-resistant, and incurable tuberculosis. *Lancet Respir. Med.* **2017**, *5* (4), 291–360.
[3]. Schiff, H. Mittheilungen aus dem Universitätslaboratorium in Pisa: Eine neue Reihe organischer Basen. *Ann. Chem. Pharm.* **1864**, *131*, 118–119.
[4]. Bharti, S. K.; Nath, G.; Tilak, R.; Singh, S. K. Synthesis, anti-bacterial and anti-fungal activities of some novel Schiff bases containing 2,4-disubstituted thiazole ring. *Eur. J. Med. Chem.* **2010**, *45*, 651–660.
[5]. Cordeiro, R.; Kachroo, M. Synthesis and biological evaluation of anti-tubercular activity of Schiff bases of 2-Amino thiazoles. *Bioorg. Med. Chem. Lett.* **2020**, *30*, 127655.
[6]. Guo, S.; Song, Y.; Huang, Q.; Yuan, H.; Wan, B.; Wang, Y.; He, R.; Beconi, M. G.; Franzblau, S. G.; Kozikowski, A. P. Identification, synthesis, and

pharmacological evaluation of tetrahydroindazole based ligands as novel antituberculosis agents. *J. Med. Chem.* **2010**, *53*, 649–659.
[7]. Santoshkumar, S.; Satyanarayana, N. D.; Anantacharya, R.; Sameer, P. Synthesis, antimicrobial, antitubercular and cheminformatic studies of 2-(1-benzofuran-2-yl)-N′-[(3Z)-2-oxo-1, 2-dihydro-3H-indol-3-ylidene] quinoline-4-carbohydrazide and its derivatives. *Int. J. Pharm. Pharm. Sci.* **2017**, *9*, 260–267.
[8]. Kumar, S.; Bawa, S.; Gupta, H. Biological activities of quinoline derivatives. *Mini Rev. Med. Chem.* **2009**, *9*, 1648–1654.
[9]. Tseng, C.-H.; Tung, C.-W.; Wu, C.-H.; Tzeng, C.-C.; Chen, Y.-H.; Hwang, T.-L.; Chen, Y.-L. Discovery of indeno[1,2-c]quinoline derivatives as potent dual antituberculosis and anti-inflammatory agents. *Molecules* **2017**, *22*, 1001.
[10]. Gaber, A.; Alsanie, W. F.; Alhomrani, M.; Alamri, A. S.; El-Deen, I. M.; Refat, M. S. Synthesis of 1-[(Aryl)(3-amino-5-oxopyrazolidin-4-ylidene) methyl]-2-oxo-1,2-dihydroquinoline-3-carboxylic Acid Derivatives and Their Breast Anticancer Activity. *Crystals (Basel)* **2021**, *11*, 571.
[11]. Salve, P. S.; Alegaon, S. G.; Sriram, D. Three-component, one-pot synthesis of anthranilamide Schiff bases bearing 4-aminoquinoline moiety as Mycobacterium tuberculosis gyrase inhibitors. *Bioorg. Med. Chem. Lett.* **2017**, *27*, 1859–1866.
[12]. Hunter, A. D. ACD/ChemSketch 1.0 (freeware); ACD/ChemSketch 2.0 and its Tautomers, Dictionary, and 3D Plug-ins; ACD/HNMR 2.0; ACD/CNMR 2.0. *J. Chem. Educ.* **1997**, *74*, 905.
[13]. Pettersen, E. F.; Goddard, T. D.; Huang, C. C.; Couch, G. S.; Greenblatt, D. M.; Meng, E. C.; Ferrin, T. E. UCSF Chimera--a visualization system for exploratory research and analysis. *J. Comput. Chem.* **2004**, *25*, 1605–1612.
[14]. Dallakyan, S.; Olson, A. J. Small-molecule library screening by docking with PyRx. *Methods Mol. Biol.* **2015**, *1263*, 243–250.
[15]. Kemmish, H.; Fasnacht, M.; Yan, L. Fully automated antibody structure prediction using BIOVIA tools: Validation study. *PLoS One* **2017**, *12*, e0177923.
[16]. Harishkumar, S.; Satyanarayan, N. D.; Santhosha, S. M. Antiproliferative and in silico admet study of new 4-(piperidin-1-ylmethyl)-2- (thiophen-2-yl) quinoline analogues. *Asian J. Pharm. Clin. Res.* **2018**, *11*, 306–313.
[17]. Aggarwal, A.; Parai, M. K.; Shetty, N.; Wallis, D.; Woolhiser, L.; Hastings, C.; Dutta, N. K.; Galaviz, S.; Dhakal, R. C.; Shrestha, R.; Wakabayashi, S.; Walpole, C.; Matthews, D.; Floyd, D.; Scullion, P.; Riley, J.; Epemolu, O.; Norval, S.; Snavely, T.; Robertson, G. T.; Rubin, E. J.; Ioerger, T. R.; Sirgel, F. A.; van der Merwe, R.; van Helden, P. D.; Keller, P.; Böttger, E. C.; Karakousis, P. C.; Lenaerts, A. J.; Sacchettini, J. C. Development of a Novel Lead that Targets M. tuberculosis Polyketide Synthase 13. *Cell* **2017**, *170*, 249-259.e25.
[18]. PyMOL. The PyMOL Molecular Graphics System, Version 2.0 Schrödinger, LLC. http://www.pymol.org/pymol (accessed January 2, 2022).
[19]. Gaillard, T. Evaluation of AutoDock and AutoDock Vina on the CASF-2013 benchmark. *J. Chem. Inf. Model.* **2018**, *58*, 1697–1706.
[20]. Cheng, F.; Li, W.; Zhou, Y.; Shen, J.; Wu, Z.; Liu, G.; Lee, P. W.; Tang, Y. admetSAR: a comprehensive source and free tool for assessment of chemical ADMET properties. *J. Chem. Inf. Model.* **2012**, *52*, 3099–3105.
[21]. Lin, J. H.; Yamazaki, M. Role of P-glycoprotein in pharmacokinetics: clinical implications: Clinical implications. *Clin. Pharmacokinet.* **2003**, *42*, 59–98.
[22]. Arthington-Skaggs, B. A.; Motley, M.; Warnock, D. W.; Morrison, C. J. Comparative evaluation of PASCO and national committee for clinical laboratory standards M27-A broth microdilution methods for antifungal drug susceptibility testing of yeasts. *J. Clin. Microbiol.* **2000**, *38*, 2254–2260.
[23]. Rocha, L.; Marston, A.; Potterat, O.; Kaplan, M. A.; Stoeckli-Evans, H.; Hostettmann, K. Antibacterial phloroglucinols and flavonoids from Hypericum brasiliense. *Phytochemistry* **1995**, *40*, 1447–1452.
[24]. MacLowry, J. D.; Jaqua, M. J.; Selepak, S. T. Detailed methodology and implementation of a semiautomated serial dilution microtechnique for antimicrobial susceptibility testing. *Appl. Microbiol.* **1970**, *20*, 46–53.
[25]. Portillo, A.; Vila, R.; Freixa, B.; Adzet, T.; Cañigueral, S. Antifungal activity of Paraguayan plants used in traditional medicine. *J. Ethnopharmacol.* **2001**, *76*, 93–98.
[26]. Maria, C. S. L.; Marcus, V. N.; de Souza. Alessandra, C. P.; Marcelle de, L. F.; Raoni S. B. G.; Thais Cristina, M. N.; Monica, A. P. Evaluation of anti-tubercular activity of nicotinic and isoniazid analogues. *ARKIVOC* **2007**, *2007*, 181–191.
[27]. Lipinski, C. A. Lead- and drug-like compounds: the rule-of-five revolution. *Drug Discov. Today Technol.* **2004**, *1*, 337–341.